Development of the SANDRA Antenna for Airborne Satellite Communication

J. Verpoorte, H. Schippers, P. Jorna, A. Hulzinga
National Aerospace Laboratory NLR
Anthony Fokkerweg 2, 1006 BM Amsterdam, the Netherlands
schipiw@nlr.nl
C. G. H. Roeloffzen, D. A. I. Marpaung
Telecommunication Engineering group, Faculty of Electrical Engineering
University of Twente, P.O. Box 217, 7500 AE, Enschede, the Netherlands
C.G.H.Roeloffzen@ewi.utwente.nl
B. Sanadgol, R. Baggen,
Department of Antennas & EM Modelling
IMST GmbH, Carl-Friedrich-Gauß Str. 2-4, 47475 Kamp-Lintfort, Germany
Bahram.Sanadgol@imst.de
Qin Wang, B. Noharet
Acreo AB, Electrum 236 , SE-164 40 Kista, Sweden
Bertrand.Noharet@acreo.se
W. Beeker, A. Leinse, R.G. Heideman
LioniX bv
P.O. Box 456, 7500 AH Enschede, the Netherlands
A.Leinse@lionixbv.nl

Abstract— Novel avionics communication systems are required for increasing flight safety and operational integrity, for optimizing economy of operations and for enhancing passenger services. One of the key technologies to be developed is an antenna system that will provide broadband connectivity within aircraft cabins at an affordable price. This paper describes the development of an electronically steered K_u-band phased array antenna with low aerodynamic profile. The antenna front-end consists of at least 1800 antenna elements, of which the beam has to be steered continuously to geostationary satellites. Best performance for the beam steering is expected from a hybrid architecture with small sub-apertures having their local own beamformers (using phase shifters). The beamformer to steer the sub-apertures of the entire antenna uses True Time Delays with an optical ring resonator. [1] [2]

TABLE OF CONTENTS

[1] 978-1-4244-7351-9/11/$26.00 ©2011 IEEE.
[2] IEEEAC paper #1658, Version 3, Updated 11 January 2011

1. INTRODUCTION

In the EC Seventh Framework Programme project SANDRA, a European consortium (lead by Selex Communications Spa, Italy) develops an integrated modular concept for a global aeronautical network and communication architecture. SANDRA is an acronym for "Seamless aeronautical networking through integration of data links, radios, and antennas". This novel avionics communication system is required for increasing flight safety and operational integrity, for optimizing economy of operations and for enhancing passenger services. One of the key technologies under development is an integrated antenna system that will enable an asymmetric high data rate link able to supply high data rate services to passengers without the high costs of installing and maintaining big radomes.

Key requirement for the SANDRA integrated antenna is the provision of broadband connectivity within aircraft cabins at an affordable price. To this end, SATCOM antennas with broadband capabilities have to be installed on aircraft. One of the key enablers is an electronically steered K_u-band phased array. K_u-band phased arrays in which the same elements are used for both transmission and reception are not possible with mature technologies. Consequently, for K_u-band two antenna arrays would be required, one for transmit and another one for reception. However the amount of data agglomerated over a range of passenger services (VoIP, Web, Email, SMS, MMS) and over a range of flights, is highly asymmetrical, with the inbound traffic being about 5 times higher than the outbound. The inbound

traffic requires the availability of a broadband K_u-band antenna in receive mode only, which is feasible. As a consequence, the focus is on the development a K_u-band receive antenna system that consists of an antenna front-end and a hybrid beam forming network. The antenna front-end will consist of at least 1800 antenna elements, of which the beam has to be steered continuously to geostationary satellites.

Cost and complexity of several antenna architectures have been studied with respect to size and performance of available RF-chips, complexity of feed-network, local oscillator network etc. Best performance for the beam steering is expected from a hybrid architecture with small sub-apertures having their local own beamformers (using phase shifters). The beamformer to steer all sub-apertures of the SANDRA antenna will consist of tuneable optical True Time Delays. In the SANDRA project [1], a consortium of companies, research institutes and universities will be developing a full scale antenna system which will be tested with aircraft modems and radios at the end of the project (2013).

This paper describes the architecture of the K_u-band antenna system with hybrid beam steering. Furthermore, the following issues related to the development of the SANDRA antenna are discussed:

- photonic broadband signal processing based on novel ring resonator principles,
- compact integrated broadband (2 GHz) antenna elements based on multilayer substrate compositions and stacked antenna radiators;
- new complex photonics combiners and integration of modulators.

The outline of this paper is as follows. Section 2 contains the system aspects of the K_u-band receive antenna. Sections 3 and 4 describe the enabling key technologies of the antenna and the state of development so far. Section 5 describes the analysis of system aspects (leading to novel overall hybrid architecture and a novel Optical Beamforming Network (OBFN)), and requirements for components: MMIC core chips, LNAs, down-converters and optical modulators. Section 6 describes the development of some essential components. The preliminary design of the multilayer structure is concisely described in section 7. Finally, the conclusions are presented in section 8.

2. SYSTEM ASPECTS

In the ITU Radio Regulations [2] portions of the K_u-band are allocated to aeronautical services:

- *AES receive band 1: 10.70 – 11.70 GHz (primary allocation to fixed satellite service)*
- *AES receive band 2: 12.50 – 12.75 GHz (primary allocation to fixed satellite service)*
- *AES transmit band: 14.00 – 14.50 GHz (secondary allocation to mobile satellite service)*

The Aeronautical Earth Stations (AES) have to comply with ITU-R RECOMMENDATION M.1643 [3] and with ETSI EN 302 186 [4], a harmonised European Norm for satellite mobile Aircraft Earth Stations (AESs) operating in the 11/12/14 GHz frequency band.

In addition, the reception of commercial satellite broadcasts is of interest:

- *Satellite TV: 11.70 – 12.50 GHz (primary allocation to broadcast satellite service)*

Satellites operating in this band are geostationary satellites spaced 2^o apart in the United States and 3^o in Europe. In order to be able to also receive these satellites at high latitudes (e.g. during inter-continental flights), the antenna system should have sufficient performance at low elevation angles.

Therefore the antenna system is required to have a small beamwidth (to discriminate between the satellite signals) and a high gain (>30 dB) also at low elevation angles. Since the gain of the antenna is related to the effective aperture of the antenna in the direction of the satellites, a conformal antenna also covering side parts of the fuselage or multiple antennas could be an advantage.

The phased array antenna shall maintain the proper (linear) polarization during all attitudes and at all positions of the aircraft (also at high latitudes). Therefore a polarization network is needed in the antenna front-end.

An antenna to be used on aircraft has to be able to operate in severe environmental conditions concerning temperature, pressure, vibration and humidity. The environmental requirements for civil airborne equipment are given in RTCA DO-160 or EUROCAE ED-14 [5].

In previous papers (see References [11] and [12]) the development of a prototype K_u-band receive antenna array has been described. This prototype phased array antenna had an instantaneous bandwidth of 2 GHz, covering the whole frequency range of 10.7 to 12.75 GHz. The enabling key technologies are the broadband K_u-band antenna elements (see Ref. [11]) and a broadband optical beam forming network (see References [7] and [12]). These key technologies are concisely described in the following section.

3. KEY TECHNOLOGIES

The total Ku-band antenna system consists of an antenna front-end and an optical beam forming network (OBFN). The output of the antenna systems is connected to a DVB-S receiver in case of reception of satellite television. A beam forming network with optical True Time Delays (TTD) is used instead of RF Phase Shifters to guarantee broadband reception (2 GHz bandwidth). The antenna elements used are stacked patch antennas.

The Antenna Front-end

The antenna front-end consists of the antenna elements and the low-noise amplification chips and down-conversion chips.

The antenna elements are stacked patch antennas. The two patches have slightly different dimensions and therefore also slightly different resonance frequencies. The combination of the two patches in one antenna element provides an antenna element that is impedance matched between 10.7 and 12.7 GHz. At least 1800 antenna elements are needed in the total antenna system (e.g. 32 tiles of 64 antenna elements resulting in an array of 2048). The tiles can be organized in a rectangular array or a circular array (an example of 24 tiles of 64 antenna elements is shown in Figure 1).

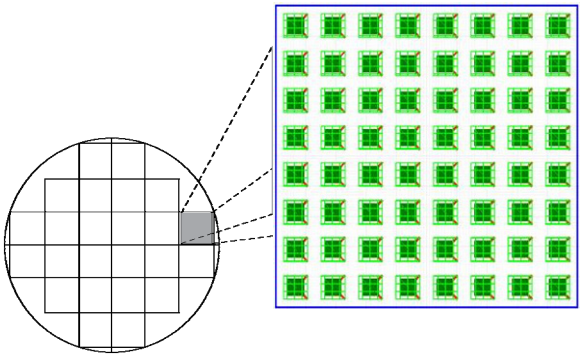

Figure 1 Example of an antenna array composed of 24 square 8x8 K_u-band building blocks crudely approximating an antenna with circular boundary

The Optical Beamforming Network (OBFN)

Optical True Time Delay (TTD) can be used to steer the beam of the phased array antenna in the entire receive band form 10.7 GHz to 12.7 GHz. The application of an OBFN in a phased array receiver system requires that the individual antenna element signals first have to be converted from the electrical to the optical domain.

In order to minimize losses, the combining of the optical signals in the OBFN is performed coherently, which requires the use of a common laser. The output light of the laser is split, and then modulated by the antenna element signals, using external modulators. The most straightforward way of doing so is to apply optical double-sideband (DSB) modulation, for example using Mach-Zehnder modulators (MZMs). The output signal of the OBFN is converted to the electrical domain by direct optical detection, using a photodiode. This is illustrated in Figure 2.

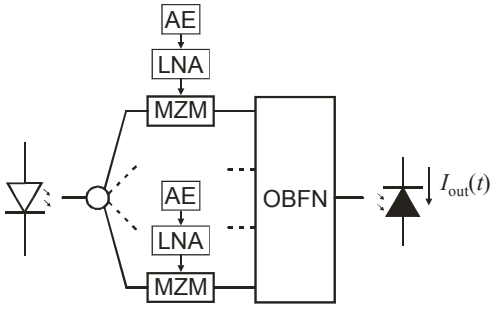

Figure 2 – Optical beamformer architecture using DSB modulation and direct detection (AE=antenna element, LNA=low-noise amplifier, MZM=Mach-Zehnder modulator, OBFN=optical beam forming network)

The spectrum of the modulated optical signal consists of the optical carrier and —depending on the modulation depth— at least two sidebands. With satellite TV operating in the 10.7–12.75 GHz band, it follows that the optical bandwidth of such a system is at least 25.5 GHz. The bandwidth of the modulated optical signal can be reduced by removing one of the sidebands (optical single-sideband (SSB) modulation). The bandwidth can be even further reduced by also removing the optical carrier, resulting in single sideband suppressed carrier (SSB-SC) modulation. The optical bandwidth then equals the RF bandwidth, which is the smallest that can be achieved without splitting the RF signals in sub-bands prior to electro-optical conversion. Optical SSB-SC modulation can be implemented in various ways [7], but the simplest way for this particular application is to use DSB modulators followed by optical sideband filters (OSBFs). DSB modulation can be performed by MZMs, which can be biased in such a way that the carrier is inherently suppressed (DSB-SC modulation) [10]. The OSBF is then only required to suppress one of the sidebands. Since the OBFN and OSBF are both linear devices, their order can be reversed, so that only one OSBF is required.

True Time Delays can be implemented by means of cascaded Optical Ring Resonators (ORR). The principle functioning of ORRs is explained in this section. The peak value of the delay of an ORR is inversely proportional to the bandwidth. This imposes a trade-off between the highest delay and the maximum bandwidth that can be obtained. To overcome this, several ORRs can be cascaded, where the total group delay response is the sum of the individual ring

responses. This is illustrated in Figure 3 and Figure 4.

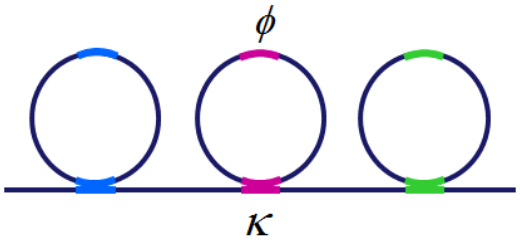

Figure 3 Cascaded optical ring resonators delay.

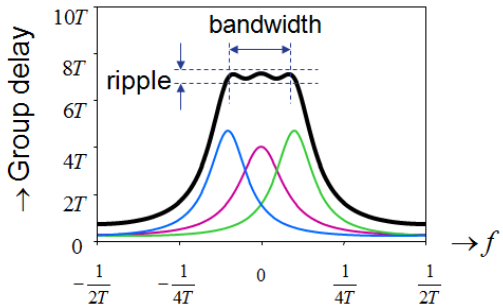

Figure 4 The group delay response of three cascaded ring resonators

A full OBFN is obtained by combining the ORR based delay elements with power splitters and combiners. An example of a 16×1 OBFN is shown in Figure 5. It is based on a binary tree topology, consisting of four sections, sixteen inputs and one output. In this particular case a total of twenty rings are involved. The rationale for using such a topology is that, for a linear PAA, increasing delay tuning ranges are required for the sixteen possible paths through the OBFN, where the upper path (from input 1 to the output) is considered as the reference path.

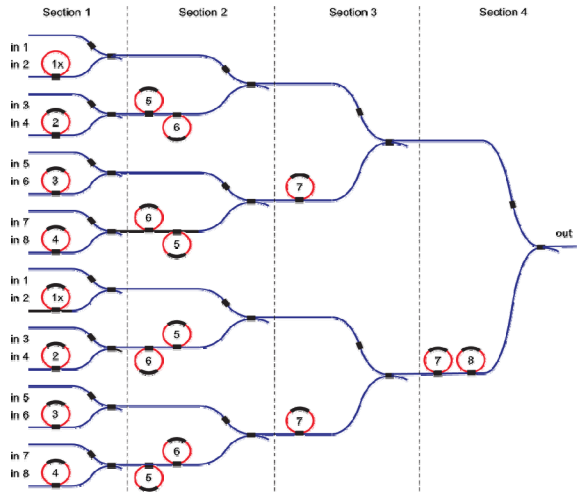

Figure 5 Architecture of an 16x1 optical beamforming network.

Details of the OBFN design can be found in Ref. [8]. A delay as high as 1.2 ns over a bandwidth of 2.5 GHz has been demonstrated with a cascade of 7 ORRs, in an 8x1 optical beamformer (see also Ref [6]). For comparison, 1 ns is approximately 30 cm of propagation distance in vacuum.

4. State of Development

A breadboard multilayer antenna has been developed that consists of a tile of 8x8 K_u-band stacked patches and a feed network with 8 combiners, where each combiner coherently sums 8 antenna elements.

The K_u-band antenna design has been optimized by using ANSOFT simulation software. The ANSOFT Designer model is shown in Figure 6. The dimensions of the patches, dog bone aperture and thicknesses of foam layers have been optimized with the aim to get an antenna which could span the frequency-band from 10.7 to 12.75 GHz. The design has a ground plane at a distance of 5 mm from the planar layer with feed traces. The function of this ground plane is to shield the antenna element from the layers below the ground plane in order to minimize the influence on the element. From a manufacturing point of view, a maximum distance of 5 mm was recommended. The computed gain of this stacked patch antenna element is about 8 dBi. Figure 7 displays the reflection coefficients of the antenna element. Notice that the return loss is below -10 dB in the frequency range between 10.7 to 12.75 GHz, as aimed, which indicates that this element has sufficiently large bandwidth for broadband data transmission. This K_u-band antenna element satisfies the preset requirements.

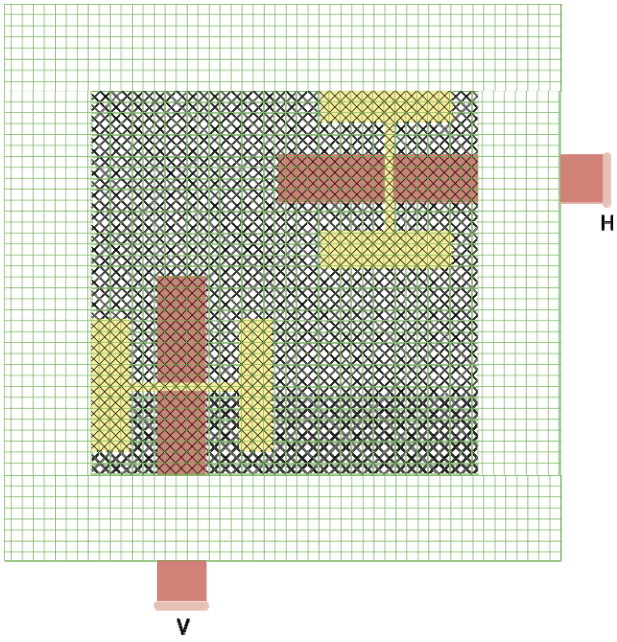

Figure 6 ANSOFT Designer model for stacked K_u-band patch antenna

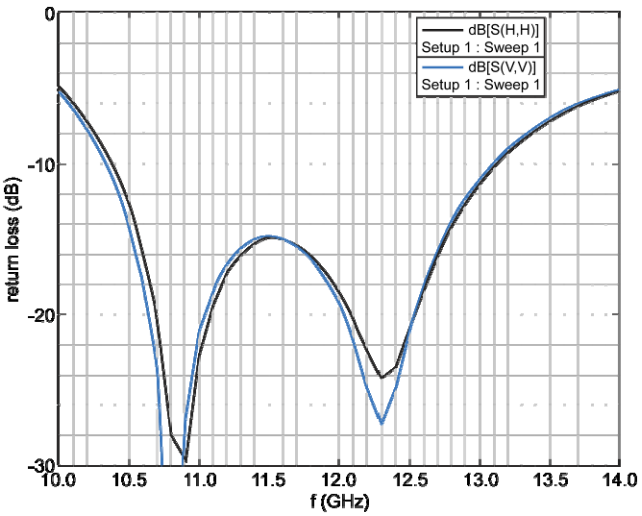

Figure 7 Reflection coefficients of stacked K_u-band patch antenna with ground plane at 5 mm distance.

A prototype 8x1 OBFN with OSBF has been manufactured and tested. The drawing of the mask file and a photo of the chip are shown in Figure 8. The beam is electronically steered by means of the 8x1 OBFN. The beam forming capabilities of antenna and OBFN have been verified for several channels in K_u-band. The prototype OBFN has been connected to the breadboard antenna. Then, The C/N ratio has been measured for frequencies in the K_u-receive band and for different antenna positions.

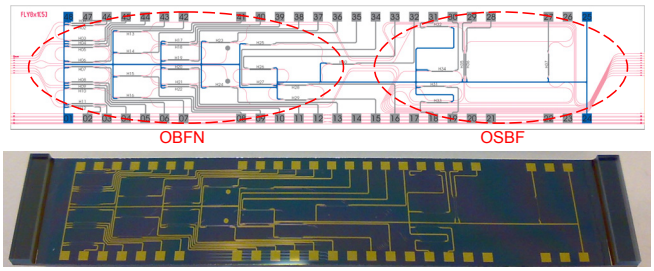

Figure 8 –Waveguide structure of the 1×8 OBFN chip and OSBF chip. (Top image: drawing of mask file; Bottom image: photo of realized device with bond pads and electrodes visible, the dimensions are 6.85 cm by 0.95 cm)

Figure 9 displays the C/N ratio for 10.7 GHz for the case that the phased array antenna is illuminated broadside, once rotated 27 degrees to the right side, and another time 27 degrees rotated to the left side, without any time delays in the beam steering. It is clearly observed that the C/N ratio decreases by about 16 dB. Obviously, beam steering is required to point the main beam into the direction of the transmitting K_u-band horn antenna. The required delay settings are based on the rotation of the antenna arrays. In the OBFN system the time delays are adjusted by tuning Mach Zehnder Interferometers by means of a heater control board.

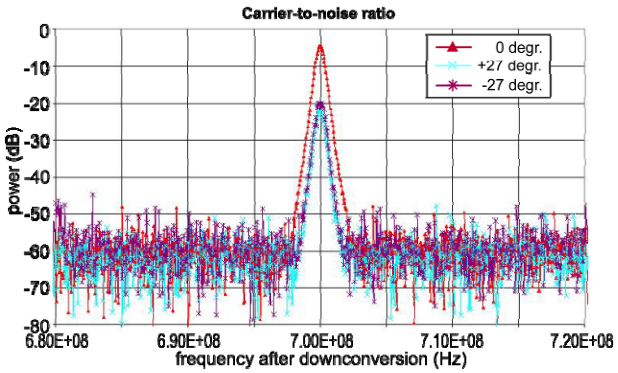

Figure 9 C/N ratio antenna array and OBFN system (no time delays); Antenna in three different positions: broadside, rotated ± 27 degrees.

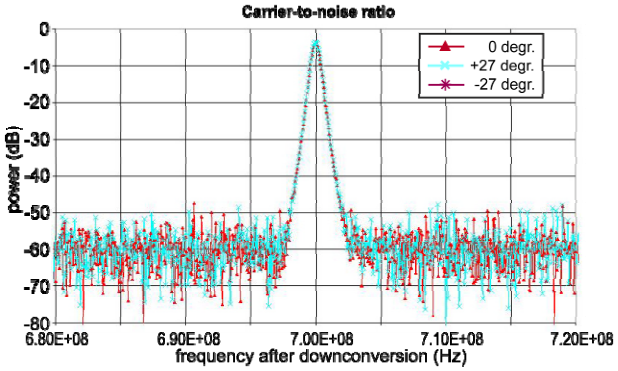

Figure 10 C/N ratio antenna array and OBFN system (adjusted time delays); Antenna in three different positions: broadside, rotated ± 27 degrees

Once the time delays have been adjusted for oblique illumination, then the main beam of the phased array antenna points once again in the direction of the transmitting antenna, and the C/N ratio remains constant when the antenna is rotated, as can be observed from Figure 10. Hence, Figure 9 and Figure 10 show clearly the properties of the beam steering capabilities of the OBFN system.

5. System Parameters

In order to receive DVB-S signals with a sufficient carrier-to-noise ratio (CNR), the number of elements in the phase array antenna should be sufficiently large. In Ref. [8] the required number of antenna elements was estimated to be at least 1800. As a consequence, an OBFN with 1800 inputs is required, which is far beyond the status of development with reference to the previous section. Therefore, we propose a two-level modular configuration as depicted in Figure 5. In this design, 32 parallel OBFN chips with 64 inputs (64 x 1) are used in the first stage and their outputs are combined by a 32 x 1 OBFN chip in the second stage. RF amplifiers are placed in the transition between the first and the second stages to achieve sufficient carrier-to-noise ratio (CNR).

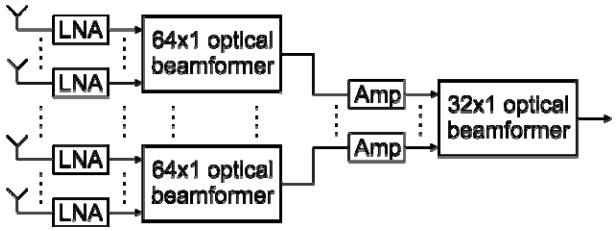

Figure 11 Two-level modular architecture of the OBFN system. LNA: low noise amplifier, Amp: second stage RF amplifier.

The performance of the phased array antenna with OBFN will strongly depend on the characteristics of the components. A preliminary system analysis has provided some specifications for antenna elements, electro-optical modulators, OBFN chips, amplifiers and Balanced Photo detectors.

Antenna elements

The K_u-band antenna elements should receive signals from satellites, with a power level in the range between -158 dBW and -152 dBW depending on the direction of arrival. Taking into account the fluctuating atmospheric conditions and changing of location, we set the requirement of the minimum detectable received power, P_{in}, to -160 dBW. For DVB-S signals with frequency range of 10.7-12.75 GHz the minimum CNR per-channel required at the input of the DVB-S receiver is 1 dB (DVB-S2 QPSK FEC=1/2), in a channel bandwidth of 33 MHz. To achieve this, suppose that a planar array with N number of elements is used together with N LNAs with a gain of 70 dB and a noise figure of 0.7 dB (T_{LNA} = 50 K). If the brightness temperature of the sky (T_{sky} = 50 K), we can calculate the minimum gain of the antenna should be in the order of 35 dBi (see Ref. [8]). Allowing a maximum scan angle of 60^o, this requires N = 1830 antenna elements. For simplification, in the rest of this document, we take N = 2048, which is a power of 2. Note that typically for this range of frequency, the inter-element spacing of the antenna elements is in the order of 1.18 cm. For an antenna with a rectangular aperture of 64 by 32 antenna elements, the dimensions of the antenna will be approximately 76 by 38 cm.

Electro-optical modulators

The specifications of the EO modulators are given with reference to the performance characteristics of MZMs.

OBFN chips

The tuning ranges of the delays that are required in the beamformers follow from the geometry of the antennas. Since the AE spacing is 1.18 cm, the maximum delay between two neighbouring elements in one row of the antennas —incorporating a maximum scan angle of 60 degrees— is roughly 34 ps. Now suppose that each OBFN has a binary tree structure as depicted inFigure 5. Then the first input port should have a fixed delay of 34 ps with respect to the second port and the second branch should have a delay element that can be tuned from 0 to 68 ps. This should be extended for the other ports, resulting in linearly increasing delay tuning ranges (up to (7x7)*34 ps = 476 ps for the 64th port). The 32 × 1 beamformer in the second stage is exactly the same, but requires fewer ports and hence a smaller maximum delay.

As for the optical losses in the OBFN chip, it is assumed that coupling losses from the laser and to the detector are in the order of 1 dB. We assume a waveguide loss of 0.05 dB/cm. Then, it can be shown that the total modulated path losses of the 64 x 1 (for each tile) and the 32 x1 OBFNs (for the complete antenna) are 0.5 dB and 3.5 dB, respectively (see Ref. [8]).

Amplifiers

The LNAs and the RF amplifiers shown in Figure 5 play an important role in the performance of the whole system. It can be shown that the optical beamformer does not degrade the performance of the receiver system in which it is applied, provided that proper amplifiers are used, and that the optical losses are kept sufficiently low. A performance analysis has shown that at least 70 dB of amplification is needed. The first LNA should have a noise figure below 0.8 dB if a margin of 10 dB is included for atmospheric attenuation. If a lower margin is used, the requirements for the noise figure of the LNA can be relaxed. The RF amplifiers at the second stage can have a less stringent noise figure to achieve the 1 dB CNR. These amplifiers are not restricted to low noise amplifiers. The actual value of the amplification depends on the size of the array, the required margin and the actual sensitivity of the optical modulators.

Laser and Balanced Photo-Detector

The laser source in the system is a distributed feedback (DFB) laser with an output optical power of 100 mW and a relative intensity noise (RIN) of -150 dB/Hz. It is assumed that the laser is temperature stabilized. The BPD has a responsivity of 0.8 A/W and a common-mode rejection ratio (CMRR) of 30 dB. The BPD output impedance is matched to 50 ohm.

The derived system parameters are summarized in Table I, below.

Table 1 Key parameters for OBFN system

Parameters	Value	Unit
Frequency range	10-7-12.75	GHz
Number of elements	2048	
Inter-element spacing	1.18	cm
Sky & AE temperatures	50 & 150	K
Received RF power	-160	dBW
Minimum CNR (33 MHz BW)	8	dB
LNA gain	70	dB
LNA noise figure	0.7	dB
Modulator insertion loss	2	dB
Modulator V_π	1.0	V
Optical waveguide loss	0.05	dB/cm
OSBF optical loss	0.25	dB
Second-stage amplification	30	dB
Input optical power	100	mW
BPD responsivity	0.8	A/W

The proposed system architecture for the optical beamforming is displayed in Figure 12.

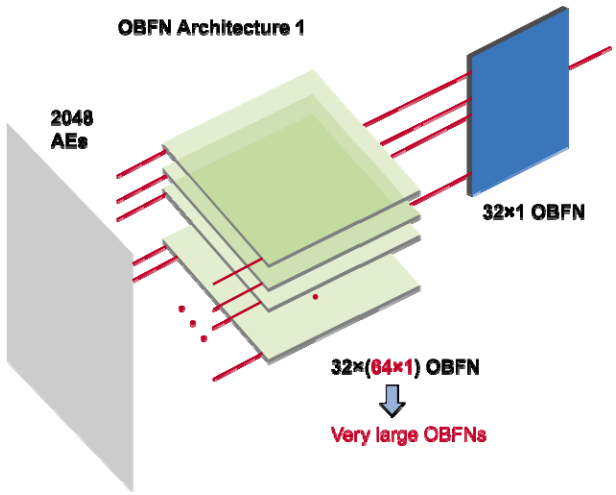

Figure 12 Proposed system architecture with 32 (64x1) OBFN at first stage;

However, the large scale of the 64 x 1 beamformer might pose a higher risk in system reliability, since the large OBFN should provide higher delay and might induce more loss. Furthermore, this system requires a large number of optical modulators (64) in one array which might lead to a low yield of the array. For this reason, we propose an alternative architecture, where RF beamforming of 4 antenna elements are performed prior to the first stage of the OBFN system (Figure 13). This will reduce the size of the OBFNs in the first stage to 16 x 1 instead of 64 x 1. These smaller OBFNs are more reliable and have already been realized and tested in previous frameworks. Moreover, the reduced number of modulators in one array (16 instead of 64) will also improve the yield. The RF beamforming prior to the OBFNs might be implemented in true-time delay elements or phase shifters.

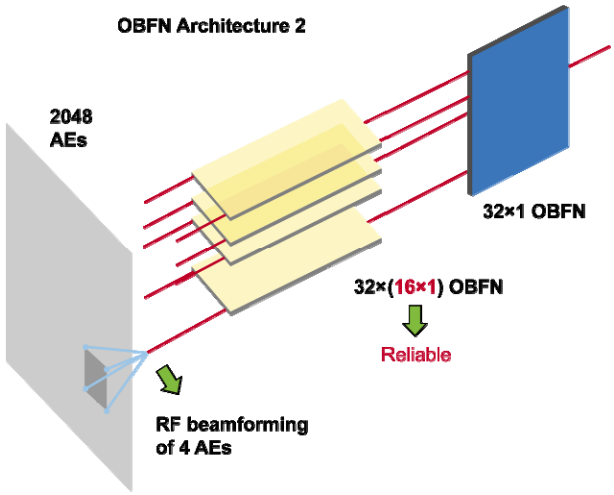

Figure 13 The alternative architecture with RF beamforming prior to the OBFN system. The first stage OBFNs are simplified into 16x1 architectures.

6. System Architecture

The antenna front-end consists of the antenna elements and the low-noise amplification and down-conversion chips.

At least 1800 antenna elements are needed in the total antenna system. The antenna consists of 32 tiles; each tile contains 4x4 sub-apertures. Each sub-aperture contains 2x2 stacked patch antenna elements. The two patches of the antenna element have slightly different dimensions and therefore also slightly different resonance frequencies. The combination of the two patches in one antenna element provides an antenna element that is impedance matched between 10.7 and 12.7 GHz. The output of each antenna element is fed to a low-noise amplifier because the signal received by only one antenna element is very weak. Before the amplified signal is fed to the optical beamforming network, it is down-converted.

Sub-arrays with RF phase shifting are used to reduce the number of channels in the optical beamforming network. The output of each sub-array (2x2) is combined and fed to a single optical channel, reducing the number of optical channels by a factor of four. Before the signals of the antenna elements are combined RF phase shifters are used.

Beam steering is performed by a cascaded optical beamforming network system. The 16 sub-apertures in one antenna tile are steered by a 16x1 OBFN. Finally, at a second stage, the signals coming from all tiles are steered by 24x1 or 32x1 OBFN depending on the final number of tiles which are required to obtain the required gain.

The complete optical beamforming architecture is shown in

Figure 14. This is a two-level modular architecture where two stages of optical beamformers are used. In Figure 14A, the phased-array antenna structure is depicted. It consists of N number of antenna tiles (here N=24 is depicted for illustrative purpose only), where each tile consists of 64 Antenna Elements (AEs) (the yellow squares in Figure 14B). Thus the total number of AEs in the system is 64xN. A monolithic microwave integrated circuit (MMIC) beamforming will be implemented to delay and combine the signals from 4 neighboring AEs. This is illustrated by the red squares in Figure 14B. This means that each tile will not have 64 RF outputs but only 16 RF outputs. These outputs will feed a 16x1 optical beamforming network (OBFN) as shown in Figure 14C. The number of 16x1 OBFNs needed is equal to the number of antenna tiles, which is N.

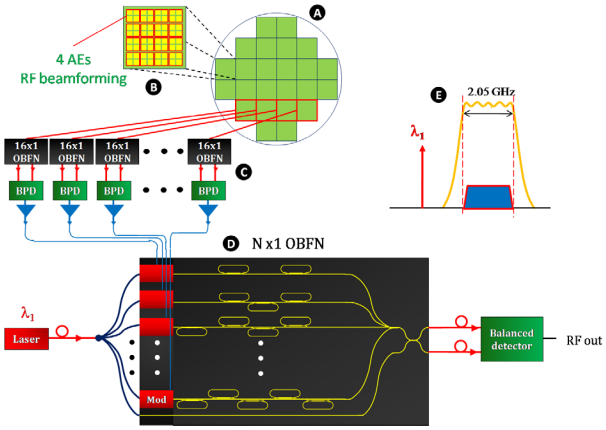

Figure 14 The complete optical beamforming system.

The 16x1 OBFN consists of a laser diode, 16 optical modulators, a 16x1 optical beamforming chip and a balanced photo-detector (BPD) to restore the RF signal. The RF output of the BPD is then amplified by a second-stage amplifier before being fed to the modulator RF inputs of the Nx1 optical beamformer, as illustrated in Figure 14D. This beamformer delays the received signals from the first stage beamformers (Figure 14E) and combines them. Here we consider RF signals with a frequency range of 10.7 GHz to 12.75 GHz, hence a 2.05 GHz bandwidth.

7. DEVELOPMENT OF COMPONENTS

The hybrid MMIC/OBFN architecture is shown in Figure 15. This architecture includes the following RF-components: Core chip, LNAs and down-converters. The development of these RF components as well as novel chips for OBFN and Electro-absorption modulators is described in this section.

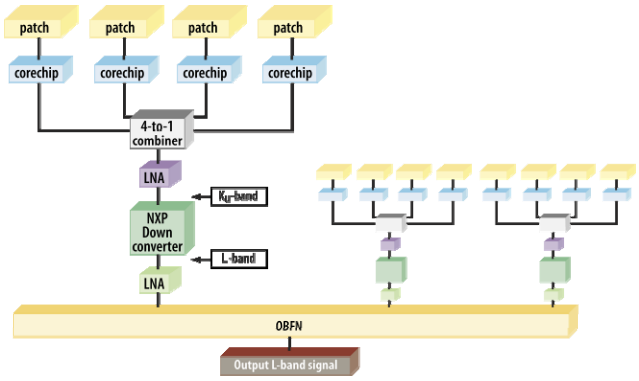

Figure 15 System architecture for K_u-band phased array antenna

Development of RF components

The upper part of the architecture in Figure 15 contains 4 patch antenna elements, which build-up one sub-aperture. The patches are combined in groups of 4 antenna elements to reduce the number of RF- and OBFN-components. For the global pointing of the sub-apertures on RF-level a so-called MMIC core-chip is used. This chip has a 4-bit phase shifter, two-stage LNA and digital steering logic on board. It has specifically been designed by IMST in cooperation with the foundry OMMIC for K_u-band reception within an ESA-project (NATALIA, see Ref. [13]) All other RF-components like K_u-band & L-band Amplifier and down-converter are off-the-shelf components.

In order to achieve 70 dB of amplification (which is required by the OBFN chip as discussed in section 5), a complete chain consisting of core-chip LNA, a separate K_u-band LNA (see Figure 15), down-converter and L-band Amplifier are designed. One major challenge is to achieve the overall amplification, and at the same time avoiding any oscillations and still retain a good noise figure (estimated 2 dB). The K_u-band components are all GaAs-based, the L-band LNA and down-converter are SiGe-based. It is expected that all components will be packaged. This will simplify the complete assembly process because one can use standard SMD-mounting techniques. One important passive component will be a typical band pass filter, required for the rejection of image frequency (placed before the down-converter). This filter will be designed as a printed structure because no suitable components could be allocated off-the-shelf.

The overall packaging density will be extremely high. For the planned module of 8x8 elements, 64 core-chips, 16 K_u-band LNAs, 16 down-converter chips, 16 L-band Amplifiers, and 16 filters have to be integrated on an area of approximately 10 cm x 10 cm. Hence, a PCB-buildup is considered where most of the digital steering signals, required by the core-chips, the complete power supply for all chips, reference signals, etc. will be located on the inner layers of the PCB. On its topside, the antenna patches are realized and on the backside all the active components and filter structures are mounted. A first layout of this backside

for a 2x2 patch array is shown in Figure 16. Please note that this is a primary layout and it will change during the course of the design. The sizes relative to each other are all to scale.

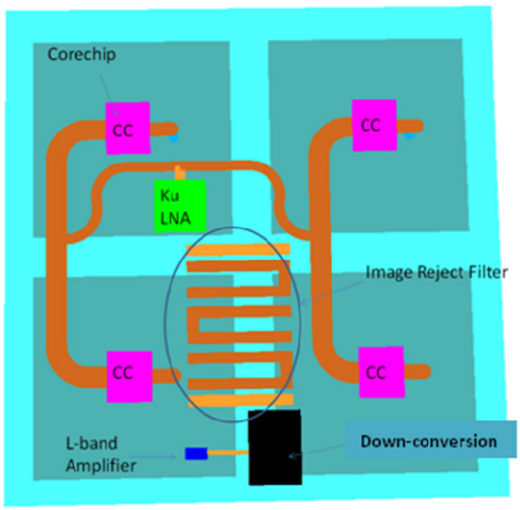

Figure 16 Lay-out structure for RF-components

From this figure it can be observed that the required space for the core-chips and the surrounding passive components is quite high. The filter could also be realized in the inner layers of the PCB. This could ease the integration of the chips and reduce the coupling. It should be noted that considering the size of one tile and the amount of amplification required, coupling will become a serious problem and, if not properly controlled, will lead to unwanted oscillations. It is planned to use complex EM-simulations to design a layout that avoids this problem.

Development of Optical Beamforming chips

In this part the progress in the design and fabrication of the optical waveguides and subsequently the basic building blocks of the OBFN chip are reported. The goal is to develop the waveguide structures to obtain the optimal settings for the OBFN chip. Several aspects are emphasized here, namely the waveguide geometry, the waveguide propagation loss, the bend loss, the optimal directional coupler geometry and the optimal ring resonator geometry.

Waveguide geometry—The waveguide consists of two layers of 170 nm Nitride separated by 500 nm oxide in between to form a parallel waveguide. The width of this guide is limited by the mono-modality criterion and by its guiding capability and limitations that stem from the production processes. An important characteristic of the waveguide is the group index of the waveguide. It is needed to determine the proper physical path length of the ring structures, which together with the group index amounts to the optical path length. The results of this calculation are shown in Figure 17.

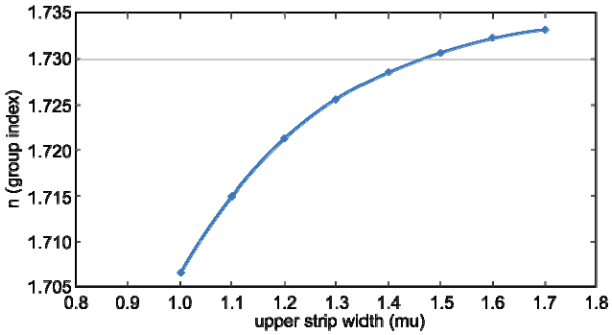

Figure 17 Calculated group index of the parallel waveguide for various widths of the upper strip of nitride

It is expected that the group index depends on the radius of curvature of the waveguide. Therefore, the group index is calculated as a function of this radius and the results are shown in Figure 18. Based on this figure it is expected that the contribution of the excess optical path length due to the sharpness of the curves can be neglected for curves with a radius > 50 µm.

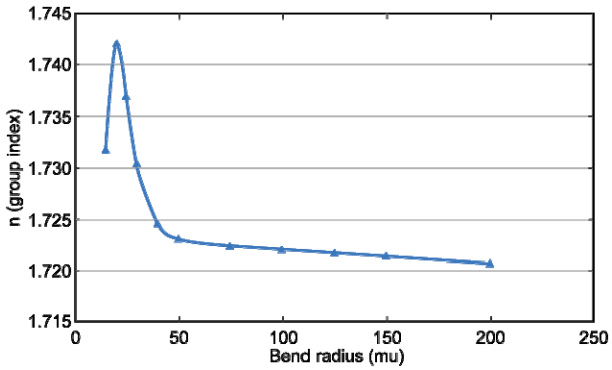

Figure 18 Calculated group index of the parallel waveguide with a upper strip width of 1.2 µm for various bend radii

Using the group index as calculated the FSR of a ring structure with a certain physical path length can be calculated. This is shown in Figure 19. As an example, the physical length of a ring with an FSR of 20 GHz needs to be 8.8 mm.

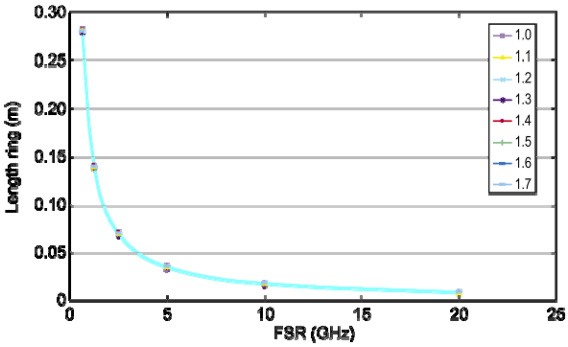

Figure 19 Calculated Free Spectral Range (FSR) of ring structures with length L for various waveguide widths.

Propagation loss —We aim for a propagation loss as low as possible with a target value of 0.05 dB/cm. Such a waveguide propagation loss can be tested using spiral shaped structures to optimize the total path length while minimizing the chip-footprint. We have chosen to use a spiral shape with a minimal bend curvature of 1 mm to exclude the influence of bend-losses to the measurement. The test structure consists of 4 of such spirals with physical path lengths of 30 cm, 40 cm, 50 cm and 60 cm. The structures are connected such that sets of them can be measured in series to extend the range of total path lengths to 110 cm, 150 cm and 180 cm by sawing the individual spirals, thereby separating them from each other. These structures are shown in Figure 20.

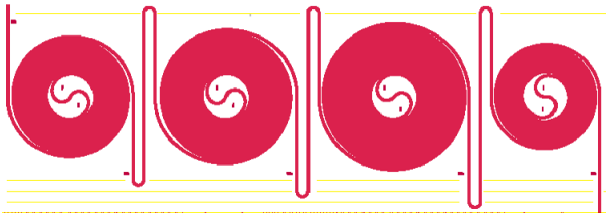

Figure 20 Four spirals

Bend loss — To reduce the footprint of the layout on the chip a bend radius as small as possible should be used. However, the losses at such a bend increase with decreasing radius. In order to find the optimum bend radius, a test structure containing several bend radii is used (Figure 21). The range of radii on the test mask is chosen as 10, 20, 50, 75, 100, 125, 150, 200 and 400 µm. For each waveguide 8 bends of 90 degrees have been placed in series.

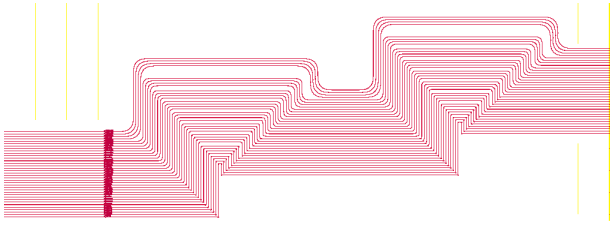

Figure 21 Bends with various radii

The measurements on the bend waveguides were also carried out. The aim is to optimize the bend radii, since sharp bends will increase the optical loss while weak bends increase the footprint of the optical chip. Measurement results in Figure 22 show that the minimum bend radius that can be achieved while the contribution of the bend loss still can be neglected is 75 microns. Below this value the bend loss starts to dominate. This value is sufficient to facilitate a small OBFN footprint.

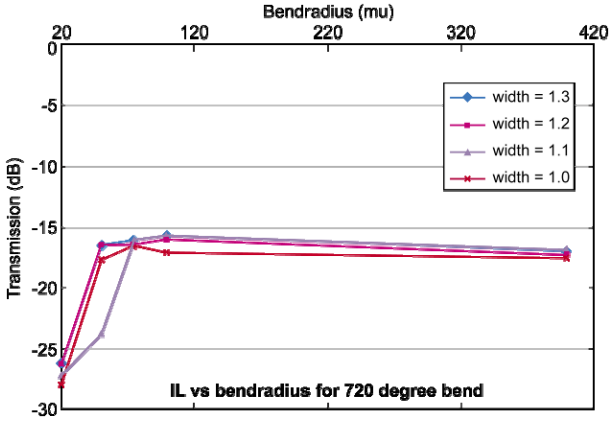

Figure 22 Measurement results of the loss of bend waveguides as function of the bend radii for various waveguide widths.

Optimal directional coupler geometry — In order to obtain a perfect 50%-50% coupling ratio in a directional coupler, a parameter range containing the relevant geometrical factors is used in the test structures. The test structures consist of 30 directional couplers for each set of waveguide width and gap size (Figure 23). The length of the straight section varies from zero to three times the 100% coupling length in equal steps. The leads (the bent sections) have been formed such that the bend radius along the propagation does not have discontinuities which we will refer to as the adiabatic shape.

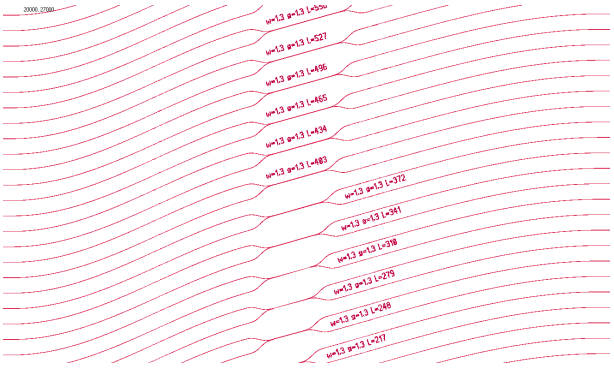

Figure 23 Directional Couplers

The directional coupler was characterized to determine the optimum length for 50%-50% coupling. Moreover a study

on reproducibility was also carried out. The results are depicted in Figure 24. The directional couplers behave as expected from numerical calculations and the measurements on two separate wafers have shown excellent reproducibility.

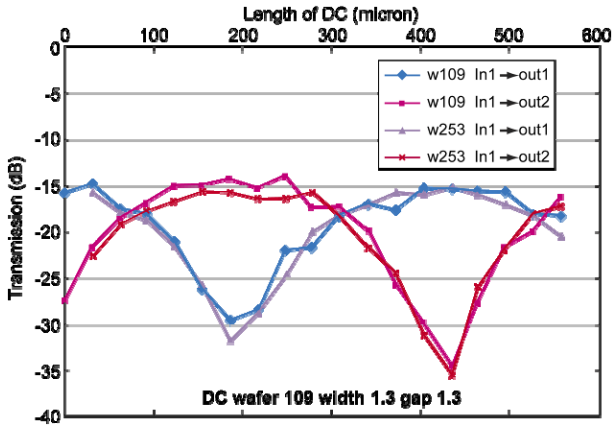

Figure 24 Measurement results on the directional couplers

Optimal ring resonator geometry — The ring resonator geometry consists of two 50% directional couplers and a ring structure with a certain total path length (Figure 25). Since the optimal design of the directional couplers has not been experimentally tested the values based on the initial calculations are used. A gap size of 1.6 µm is used and the corresponding length of the straight section per waveguide based on table 1 (the length to obtain 50% is half of the length to obtain 100%) are used in the design. The ring is designed to have an FSR of 20 GHz to facilitate the characterization in the measurement setup. The straight section in between the directional couplers is set to 2.2 mm to provide sufficient length for the heater. In the test mask both a ring resonator with and without a drop port have been included.

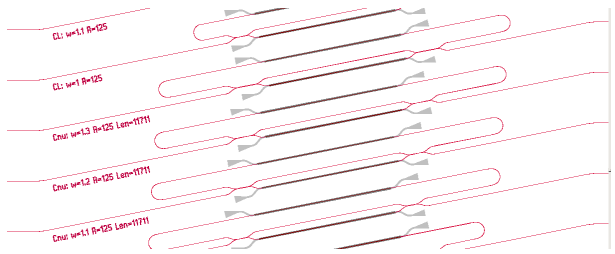

Figure 25 Ring resonator structure

Various measurements were performed on the optical ring resonators. The aim is to determine the loss of the optical waveguides expressed in dB/cm. A propagation loss as low as 0.2 dB/cm for TE polarized light has been achieved. This loss is within the target value calculated from the system level simulation. This result demonstrates the feasibility of producing a low loss OBFN chip. The details of these loss measurements will be reported elsewhere.

Development of electro-absorption modulators

The output light of the laser in Figure 14 is split, and then modulated by the antenna element signals using external modulators. These devices modulate the intensity of a laser beam via an electric voltage. For modulators in telecommunications small size and modulation voltages are desired. The Electro-Absorption Modulator (EAM) is suitable for use in modulation links in telecommunications. Most EAM are made in the form of a waveguide with electrodes for applying an electric field in a direction perpendicular to the modulated light beam. For achieving a high extinction ratio, the quantum confined Stark effect in a vertical pin diode structure is exploited for the development of in the modulators to be used in the OBFN system here. Compared with Electro-optic modulator (EOM), EAM can operate with much lower voltages (a few volts instead of ten volts or more). They can be operated at very high speed; a modulation bandwidth of tens of gigahertz can be achieved, which makes these devices useful for the OBFN.

The modulators under development exploit surface normal multiple quantum wells. Compared to traditional waveguide electro-absorption modulators, surface-normal modulators offer significant advantages in terms of polarisation insensitivity, large active apertures and low insertion losses. Arrays of surface-normal modulators can be made with high modulator counts, and passive alignment can be used to couple light between the modulator array and other optical elements.

The modulation speed of EAM is usually RC-limited. The capacitance C of EAM can be estimated by using the following thin-plate capacitance model:

$$C = \frac{\varepsilon \varepsilon_r A}{d}$$

where d is the intrinsic region thickness and A the active area of the modulator. There is therefore a clear design trade-off between modulation speed and modulator aperture. Thicker active areas also contribute to lower capacitance and therefore higher speed, as well as stronger absorption coefficient, while they also require higher voltage swings to drive the modulator. Depending on the size of the modulator, typical modulation speed of surface-normal EAM lies in the kHz-GHz range, with reported record speeds of 37GHz for modulators with a few µm in diameter (see Ref. [14]).

Acreo (Kista, Sweden) has fabricated discrete modulators (see Figure 26) based on InGaAs/InAlAs coupled quantum wells (see Ref. [15]), which operate at 1550 nm. Typical values for contrast ratio, insertion loss, voltage swing, optical and electrical bandwidths are 2:1, 5 dB, 3 V, 20 nm and 1 GHz respectively for modulators with 100µm aperture.

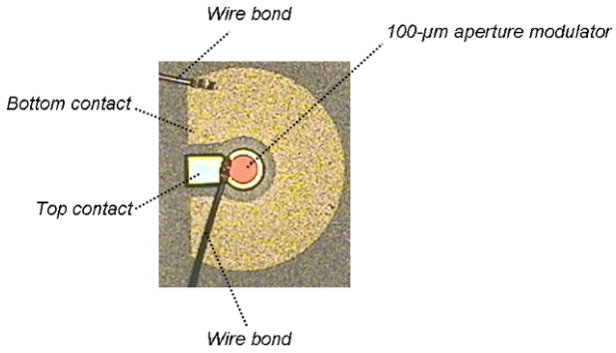

Figure 26 Photo of a fabricated 100µm aperture modulator

Smaller modulators are being developed to match the modulator speed to the K_u-band. 16-modulator arrays will be fabricated according to process steps, including:

- Mesa formation by photolithography and wet or dry etching.
- Creation of p and n contacts
- Deposition of a metallic mirror
- Flip-chip bonding on a passive interconnect carrier
- Substrate removal

8. CONCLUSIONS

In this paper the development of airborne K_u-band phased array antenna system for receive of DVB-S signals has been described. In the SANDRA project [1] a full scale antenna system which will be tested with aircraft modems and radios at the end of the project (2013). The beam steering in the phased array antenna is performed by a combination of RF phase shifters and optical chips using ring resonators. The RF phase shifters are used the global pointing of the sub-apertures. A cascaded optical beam forming network system is used for fine beam steering. On antenna tile level, the 16 sub-apertures are steered by a 16x1 OBFN. At a second stage, the signals coming from all tiles are steered by 24x1 or 32x1 OBFN depending on the final number of tiles. Some essential novel components for the beam steering are: MMIC core chips for RF beam steering of antenna elements in sub-arrays, Optical Beamforming chips and Electro-Absorption Modulators. The development of these novel components has been described in Section 7.

The phased array antenna with the proposed architecture will be built by a consortium consisting of University of Twente (responsible for the optical beamforming network design), Lionix BV (responsible for the design and manufacturing of the optical beamforming chip), ACREO (responsible for the design and manufacturing of the optical modulators), IMST (responsible for the design of the RF front-end), EADS IW (FR) and NLR (responsible for the design of the phased array antenna) and Cyner B.V (responsible for the manufacturing of the antenna and RF PCBs). Alenia Aeronautica will assist in deriving the environmental requirements for the airborne antenna system. Thales Aerospace (UK) will be managing the project.

ACKNOWLEDGEMENT

The research leading to these results has been partially funded by the European Community's Seventh Framework Programme (FP7/2007-2013) under Grant Agreement n° 233679. The SANDRA project is a Large Scale Integrating Project for the FP7 Topic AAT.2008.4.4.2 (Integrated approach to network centric aircraft communications for global aircraft operations). The project has 31 partners and started on 1st October 2009.

REFERENCES

[1] SANDRA (Seamless Aeronautical Networking of Datalink, Radios and Antennas), DG RTD Aeronautics 7th Framework Programme, Grant Agreement n° 233679. Project Starting Date: October, 1st, 2009.

[2] The Radio Regulations, edition of 2004, contain the complete texts of the Radio Regulations as adopted by the World Radio-communication Conference (Geneva, 1995) (WRC-95) and subsequently revised and adopted by the World Radio-communication Conference (Geneva, 1997) (WRC-97), the World Radio-communication Conference (Istanbul, 2000) (WRC-2000), and the World Radio-communication Conference (Geneva, 2003) (WRC-03) including all Appendices, Resolutions, Recommendations and ITU-R Recommendations incorporated by reference.

[3] RECOMMENDATION ITU-R M.1643, Technical and operational requirements for aircraft earth stations of aeronautical mobile-satellite service including those using fixed satellite service network transponders in the band 14-14.5 GHz (Earth-to-space), 2003

[4] ETSI EN 302 186 v1.1.1 (2004-01); Satellite Earth Stations and Systems (SES); Harmonised European Norms for satellite mobile Aircraft Earth Stations (AESs) operating in the 11/12/14 GHz frequency bands covering essential requirements under article 3.2 of the R&TTE directive

[5] EUROCAE ED-14E; Environmental Conditions and Test procedures for Airborne Equipment, March 2005.

[6] L. Zhuang, C. G. H. Roeloffzen, R. G. Heideman, A. Borreman, A. Meijerink, W. van Etten, "Single-chip ring resonator-based 1 × 8 optical beam forming network in CMOS-compatible waveguide technology," IEEE Photon. Technol. Lett., vol. 15, no. 15, pp. 1130–1132, Aug. 2007.

[7] A. Meijerink, C. G. H. Roeloffzen, L. Zhuang, D. A. I. Marpaung, R. G. Heideman, A. Borreman, W. van Etten, "Phased array antenna steering using a ring resonator-based optical beam forming network," Proc. 13th IEEE/CVT Symp. Benelux, Liège, Belgium, 23 Nov. 2006, pp. 7–12.

[8] A. Meijerink, C. G. H. Roeloffzen, R. Meijerink, L. Zhuang, D. A. I. Marpaung, M.J. Benthum, M. Burla, J. Verpoorte, P. Jorna, A. Hulzinga , W. van Etten. "Novel ring resonator-based integrated photonic beamfomer for broadband phased-array receive antennas – part I: design and performance analysis", Journal Lightwave Technol., Vol. 28, No.1, pp. 3-18, Jan. 2010.

[9] L. Zhuang, A. Meijerink, C. G. H. Roeloffzen, D. A. I. Marpaung, J. Peña Hevilla, W. van Etten, R. G. Heideman, A. Leinse, M. Hoekman, "Phased array receive antenna steering using a ring resonator-based optical beam forming network and filter-based optical SSB-SC modulation," Proc. International Topical Meeting on Microwave Photonics (MWP'2007), Victoria, BC, Canada, Oct. 3-5, 2007, pp. 88-91.

[10] R. Montgomery, R. DeSalvo, "A novel technique for double sideband suprressed carrier modulation of optical fields," IEEE Photon. Technol. Lett., vol. 7, no. 4, pp. 434–436, Apr. 1995.

[11] H. Schippers, J. Verpoorte, P. Jorna, A. Hulzinga, A. Meijerink, C. G. H. Roeloffzen, L. Zhuang, D. A. I. Marpaung, W. van Etten, R. G. Heideman, A. Leinse, A. Borreman, M. Hoekman M. Wintels, "Broadband Conformal Phased array with Optical Beamforming for Airborne Satellite Communication", Proc. of the IEEE Aerospace Conference, March 2008, Big Sky, Montana, US.

[12] H. Schippers, J. Verpoorte, P. Jorna, A. Hulzinga, L. Zhuang, A. Meijerink, C. G. H. Roeloffzen, D. A. I. Marpaung, W. van Ettten, R. G. Heideman, A. Leinse, M. Wintels, "Broadband Optical Beam Forming for Airborne Phased Array Antenna", Proc. of the IEEE Aerospace Conference, March 2009, Big Sky, Montana, US.

[13] S. Vaccaro, D. Llorens del Río, R. Torres Sánchez, R. Baggen, "Low cost phased array for mobile K_u-band satellite terminal", *4th European Conference on Antennas and Propagation EuCAP*, Barcelona, Spain, April 2010.

[14] C. C. Barron, C. J. Mahon, B. J. Thibeault, G. Wang, W. Jiang, L. A. Coldren, and J. E. Bowers, "Millimeter-wave asymmetric Fabry–Perot modulators," IEEE J. Quantum Electron., vol. 31, pp. 1484–1493, Aug. 1995.

[15] Q. Wang, B. Noharet, S. Junique, S. Almqvist, D. Algren, J.Y. Andersson, "1550 nm transmissive/ reflective surface-normal electro-absorption modulator arrays", Electron. Lett. Volume 42, Issue 1, p.47–49, 2006.

BIOGRAPHIES

Jaco Verpoorte was born in the Netherlands in 1966 and studied Electrical Engineering at the Eindhoven University of Technology where he received a M.Sc. degree in 1991. After his study he joined the National Aerospace Laboratory NLR in Marknesse where he is still working as an R&D Manager in the field of Electromagnetic Technology. His current research activities include Electromagnetic Compatibility, Antennas and Satellite Navigation.

Harmen Schippers is senior scientist at the National Aerospace Laboratory NLR. He received his Ph. D. degree in applied mathematics from the University of Technology Delft in 1982. Since 1981 he has been employed at the National Aerospace laboratory NLR. He has research experience in computational methods for aero-eleastics, aeroacoustic and electromagnetic problems. His current research activities are development of technology for integration of smart antennas in aircraft structures, and development of computational tools for installed antenna analysis on aircraft and spacecraft.

Adriaan Hulzinga *received his BEng degree in electronics from the Hogeschool Windesheim in Zwolle. Since 1996 he has been employed at the National Aerospace laboratory (NLR) as a senior application engineer. He is involved in projects concerning antennas and Electromagnetic compatibility (EMC).*

Pieter Jorna *received the M.Sc. degree in applied mathematics from the University of Twente in 1999. From 1999 to 2005 he was with the Laboratory of Electromagnetic Research at the University of Technology Delft. In 2005 he received the Ph.D. degree for his research on numerical computation of electromagnetic fields in strongly inhomogeneous media. Since 2005 he is with the National Aerospace Laboratory (NLR) in the Netherlands as R&D engineer.*

Chris G. H. Roeloffzen *was born in Almelo, The Netherlands, in 1973. He received the MSc degree in applied physics and PhD degree in electrical engineering from the University of Twente, Enschede, The Netherlands, in 1998 and 2002, respectively. From 1998 to 2002 he was engaged with research on integrated optical add-drop demultiplexers in Silicon Oxinitride waveguide technology, in the Integrated Optical MicroSystems Group at the University of Twente. In 2002 he became an Assistant Professor in the Telecommunication Engineering Group at the University of Twente. He is now involved with research and education on optical fiber communications systems. His current research interests include optical communications and RF photonic signal processing techniques.*

David A. I. Marpaung *was born in Balikpapan, Indonesia in 1979. He received the B.Sc. degree in physics (with honours) from Institut Teknologi Bandung, Indonesia, in 2002, and the M.Sc. degree in applied physics and the Ph.D. degree in electrical engineering, both from the University of Twente, Enschede, The Netherlands, in 2003 and 2009, respectively. From 2005 to 2009 he was working on his Ph.D. research on performance enhancements of analog photonic links in the Telecommunication Engineering group, University of Twente. From July to October 2008 he was a guest researcher at the Netherlands Foundation for Research in Astronomy (ASTRON) working on gain enhancement and noise figure reduction of externally modulated analog photonic links, which will be used in a large-scale phased array antenna for radio astronomy purposes. He is now working as a postdoctoral researcher in the Telecommunication Engineering group, carrying out research on a large-scale photonic beamformer based on optical ring resonators. Dr. Marpaung is a member of the Photonics Society of the IEEE.*

Bahram. Sanadgol *has received his Master of Science in Electrical and Electronics Engineering from University of Duisburg-Essen (Germany), in April 2007. Since November 2005 he joined the Antenna and EM-Modelling department of IMST. His research work focuses on phased-array design, simulation methods for planar arrays, and advanced measurement techniques for antennas.*

Rens Baggen *was graduated from the Technical University of Eindhoven in 1992 with emphasis on antennas and propagation, and started working at the Dutch Aerospace Laboratory (NLR) in Amsterdam in 1993. There he worked in the fields of avionics and quality management. In 1995 he joined the department of Antennas & EMC of the IMST and specialised in antenna theory, simulation methods and tools, waveguide antennas, meta-materials and measurement techniques, amongst others. Phased array technology is one of his main topics. His work involves also management and acquisition and coordination/management of long term EU- and European Space Agency-projects.*

Willem P. Beeker *received the M.Sc. degree in applied physics from the University of Twente, Enschede, The Netherlands in 2004. In 2010 he received the Ph.D. degree at the same university for his research in the field of nonlinear optics. In 2009 he joined LioniX BV where he is now involved as a design engineer in several integrated optics projects.*

Arne Leinse *was born in Enschede, the Netherlands, in 1977 and studied applied physics at the University of Twente where he received a M.Sc. degree at the integrated Optical Microsystems group in 2001. In this same group he started his PhD work on the topic of active microring resonators for various optical applications. His PhD work was carried out in the framework of a European project (IST 2000-28018 "Next generation Active Integrated optic Sub-systems") and his thesis was titled: "Polymeric microring resonator based electro-optic modulator". In 2005 he joined LioniX BV where he is now involved as a project engineer in several integrated optical projects.*

René G. Heideman *was born in Goor, The Netherlands, in 1965. He received the M.Sc. and Ph.D. degrees in applied physics from the University of Twente, Enschede, The Netherlands, in August 1988 and January 1993, respectively. After his Postdoc positions he applied his extensive know-how in the industry. Since 2001, he has been co-founder and CTO of LioniX B.V., Enschede, The Netherlands. He is an expert in the field of microsystem technology, in which he has more than twenty years of experience. He specializes in integrated optics, covering both (bio-)chemical sensing and telecom applications. He is (co)author of more than 100 papers, and holds more than twenty patents in the integrated optics field, on ten different subjects. Dr. Heideman participates in the Dutch IOP steering committee as well as several European projects.*

Bertrand Noharet, *born 1969, received his engineering degree in physics in 1992 from the Ecole Nationale Supérieure de Physique de Marseille, France, and his PhD in optoelectronics from the University of Saint-Etienne, France, in 1996. From 1993 to 1995, Bertrand Noharet has been involved as a research engineer at Thales Research and Technology (formerly Thomson-CSF Corporate Research Centre), Orsay, in the development of optical fibre sensors for the control of civil engineering structures. Since 1995, he has been with Acreo, where he has participated in and coordinated several national and international projects on optical information processing systems. He is currently senior project manager in charge of the optoelectronics activities at Acreo, with a special focus on nanophotonics for telecommunication and imaging.*

Qin, Wang *received Licentiate and Ph.D. degrees in solid state physics at Lund University in Sweden, in 1996 and 1999, respectively. Her research fields at Lund focused on electron transport physics in nanoelectronic devices based on quantum dots and quantum wires. Now she is a senior research scientist at Acreo in Sweden, and working on high performance optoelectronic devices including photodetectors, lasers, amplifiers, modulators and sensors based on InP, GaAs GaSb, and GaN III-V low dimensional quantum structures for imaging, telecommunication and optical information processing applications. She is currently involved in the device design, fabrication, monolithic or hybridization integration and characterization techniques. She has participated in several European projects, for example, Q-switch, Labels, Iphobac and Sandra projects.*